0026-895X/06/6903-727–736$20.00
MOLECULAR PHARMACOLOGY
Copyright © 2006 The American Society for Pharmacology and Experimental Therapeutics
Mol Pharmacol 69:727–736, 2006

Vol. 69, No. 3
17715/3087360
Printed in U.S.A.

A Membrane-Permeable Peptide Containing the Last 21 Residues of the $G\alpha_S$ Carboxyl Terminus Inhibits G_S-Coupled Receptor Signaling in Intact Cells: Correlations between Peptide Structure and Biological Activity

Anna Maria D'Ursi, Laura Giusti, Stefania Albrizio, Francesca Porchia, Cinzia Esposito, Gabriella Caliendo, Claudia Gargini, Ettore Novellino, Antonio Lucacchini, Paolo Rovero, and Maria Rosa Mazzoni

Dipartimento di Psichiatria, Neurobiologia, Farmacologia e Biotecnologie, Università di Pisa, Pisa, Italy (C.G., L.G., A.L., M.R.M., F.P.); Dipartimento di Scienze Farmaceutiche, Università di Salerno, Fisciano (Sa), Italy (A.M.D., C.E.); Dipartimento di Chimica Farmaceutica e Tossicologica, Università di Napoli "Federico II", Napoli, Italy (S.A., G.C., E.N.); and Laboratorio di Chimica e Biologia di Peptidi e Proteine, Dipartimento di Scienze Farmaceutiche, Università di Firenze, Sesto Fiorentino (Fi), Italy (P.R.)

Received August 5, 2005; accepted December 5, 2005

ABSTRACT

Cell-penetrating peptides are able to transport covalently attached cargoes such as peptide or polypeptide fragments of endogenous proteins across cell membranes. Taking advantage of the cell-penetrating properties of the 16-residue fragment penetratin, we synthesized a chimeric peptide that possesses an N-terminal sequence with membrane-penetrating activity and a C-terminal sequence corresponding to the last 21 residues of $G\alpha_s$. This $G\alpha_s$ peptide was an effective inhibitor of 5′-*N*-ethylcarboxamidoadenosine (NECA) and isoproterenol-stimulated production of cAMP in rat PC12 and human microvascular endothelial (HMEC-1) cells, whereas the carrier peptide had no effect. The maximal efficacy of NECA was substantially reduced when PC12 cells were treated with the chimeric peptide, suggesting that it competes with $G\alpha_s$ for interaction with receptors. The peptide inhibited neither G_q- nor G_i-coupled receptor signaling. The use of a carboxy-fluorescein derivative of the peptide proved its ability to cross the plasma membrane of live cells. NMR analysis of the chimeric peptide structure in a membrane-mimicking environment showed that the $G\alpha_s$ fragment assumed an amphipathic α-helical conformation tailored to make contact with key residues on the intracellular side of the receptor. The N-terminal penetratin portion of the molecule also showed an α-helical structure, but hydrophobic and hydrophilic residues formed clustered surfaces at the N terminus and center of the fragment, suggesting their involvement in the mechanism of penetratin internalization by endocytosis. Our biological data supported by NMR analysis indicate that the membrane-permeable $G\alpha_s$ peptide is a valuable, nontoxic research tool to modulate G_s-coupled receptor signal transduction in cell culture models.

G protein-coupled receptors (GPCRs) represent a large family of cell-surface receptors sharing a common transmembrane structure and signal transduction mechanisms. The basic unit of GPCR signaling is composed of a heptahelical receptor, a heterotrimeric GTP-binding protein (G protein), and an effector, such as an enzyme or an anion channel. The binding of an agonist ligand to the GPCR changes its conformation to allow productive coupling with its cognate G protein, leading to the exchange of GTP for GDP on the $G\alpha$ subunit and consequent dissociation of $G\alpha$-GTP from the $G\beta\gamma$ complex.

Multiple sites of interaction cooperate in the physical coupling between the activated receptor and the G protein (Cabrera-Vera et al., 2003). Data from crystallographic, biochemical, and mutagenesis studies indicate that the key

This work was supported by Ministero dell'Istruzione, dell'Universitá e della Ricerca grants (to A.L. and M.R.M.) and by a grant from Fondazione Ente Cassa di Risparmio di Firenze (to P.R.).

A.M.D. and L.G. contributed equally to this work.

Article, publication date, and citation information can be found at http://molpharm.aspetjournals.org.
doi:10.1124/mol.105.017715.

ABBREVIATIONS: GPCR, G protein-coupled receptor; $G\alpha_s(374–394)C^{379}A$, a synthetic peptide corresponding to those residues of $G\alpha_s$ with a cysteine substituted by an alanine; DQF-COSY, double-quantum filter correlation spectroscopy; TOCSY, total correlation spectroscopy; NOESY, nuclear Overhauser spectroscopy; DPC, dodecyl phosphocholine; NECA, 5′-*N*-ethylcarboxamidoadenosine; HMEC-1, human microvascular endothelial cell; PBS, phosphate-buffered saline; FBS, fetal bovine serum; F12K, Kaighn's modified Ham's F12 medium.

elements of the interaction are primarily the second and third intracellular loops of the receptor making physical contact with the C terminus of the Gα subunit (Kobilka et al., 1988; Kostenis et al., 1997). The last ~50 residues of the Gα subunits play a central role in discriminating between different receptor subtypes or different functional states of the same receptor (Cabrera-Vera et al., 2003; Havlickova et al., 2003; Slessareva et al., 2003).

Pharmacological agents that act as agonists or antagonists of GPCRs are the most common type of drug in clinical use today. Irrespective of their chemical structure, all of these agents have a common mechanism of action in that they act extracellularly either to mimic or to preclude agonist binding to its receptor. As an alternative approach to antagonism of GPCR signaling, the receptor-G protein interface can be targeted with agents that block coupling between the receptor and the G protein intracellularly. Such an approach is expected to produce G protein-specific rather than receptor-specific antagonism. This strategy has produced several successful results using polypeptides derived from either the putative contact surface on the receptor or the Gα subunit (Freissmuth et al., 1999).

In intact cells, membrane-permeable peptides containing the C-terminal sequence of $G\alpha_q$ and $G\alpha_s$ disrupt 5-hydroxytryptamine 2c and β_2-adrenergic receptor-mediated activation of phospholipase C-β and adenylyl cyclase, respectively (Chang et al., 2000). Cellular expression of a 83-residue polypeptide derived from the C terminus of $G\alpha_s$ inhibits β_2-adrenergic and dopamine D_{1A} receptor-mediated cAMP production (Feldman et al., 2002). Minigene plasmids encoding oligopeptides representing the last 11 C-terminal residues of $G\alpha_i$, $G\alpha_o$, $G\alpha_q$, $G\alpha_{12}$, and $G\alpha_{13}$ have been successfully used to discern the contribution of different G proteins to signaling by M_2 muscarinic and thrombin receptors (Gilchrist et al., 1999; Vanhauwe et al., 2002).

In a previous article (Mazzoni et al., 2000), we showed that a 21-residue synthetic peptide, $G\alpha_s(374–394)C^{379}A$, derived from rat $G\alpha_s$ C terminus inhibits A_{2A} adenosine receptor-mediated activation of adenylyl cyclase in rat striatal membranes, and it acquires a defined helical conformation in solution. Here, we present both biological and structural data of a membrane-permeable synthetic peptide containing the sequence of the $G\alpha_s(374–394)C^{379}A$ peptide on the C-terminal side. This membrane-permeable peptide was designed using as carrier molecule, penetratin, a 16-residue fragment derived from the homeodomain of the *Drosophila melanogaster* transcription factor Antennapedia that translocates through biological membranes (Derossi et al., 1994). The membrane-permeable 37-residue peptide (dubbed A42) was able to cross HMEC-1 and PC12 cell plasma membrane inhibiting A_{2A}, A_{2B} adenosine, and β-adrenergic receptor-stimulated cAMP production without affecting G_q- and G_i-coupled receptor signaling. Structural data indicated the molecular basis of A42 tropism for plasma membrane. According to previous conformational studies of isolated penetratin (Lindberg et al., 2001) and $G\alpha_s$ fragments (Mazzoni et al., 2000), both A42 segments were arranged in α-helical structures so that the presence of one did not affect the conformation and functionality of the other. Our synthetic peptide represents a powerful tool to inhibit G_s-coupled receptor signaling in intact cells.

Materials and Methods

Adenosine deaminase was obtained from Roche Molecular Biochemicals (Mannheim, Germany). Fetal bovine serum (FBS) was from Cambrex Corporation (East Rutherford, NJ). MCDB 131 medium was purchased from Invitrogen (Carlsbad, CA). Kaighn's modified Ham's F12 medium (F12K), penicillin, streptomycin, horse serum, papaverine, 5′-*N*-ethylcarboxamidoadenosine (NECA), isoproterenol, forskolin, and direct cAMP enzyme immunoassay kit (CA-200) were products of Sigma-Aldrich (St. Louis, MO). 2,4-Difluoro-α-α[1]-bis(1*H*-1,2,4–triazol-1ylmethyl)benzyl alcohol (fluconazole) was a product of Pfizer Inc. (New York, NY). All other reagents were from standard commercial sources and were of the highest grade available.

Cell Culture. PC12 cells obtained from the American Type Culture Collection (Manassas, VA) were maintained in F12K medium supplemented with 15% horse serum, 2.5% FBS, 100 units/ml penicillin, 100 μg/ml streptomycin, and 0.02 mg/ml fluconazole in an atmosphere of 95% air/5% CO_2 at 37°C. Cells were recultivated two to three times per week. A human dermal microvascular endothelial cell line that was transformed using SV-40 was also used (HMEC-1; obtained from Dr. E. Ades, Centers for Disease Control and Prevention, Atlanta, GA). Cells were maintained in MCDB 131 medium supplemented with 5% FBS, penicillin/streptomycin (5000 units/ml and 5000 μg/ml, respectively), hydrocortisone (500 μg/ml), epidermal growth factor (0.01 μg/ml), and L-glutamine (2 mM) at 37°C as above. Cells were seeded at 1×10^5 cells/ml and were subcultured at confluence. In our studies, cells were used at passages 18 to 24.

To determine the number of viable PC12 cells in proliferation, a colorimetric assay was used (CellTiter 96 AQ_{ueous} One Solution Cell Proliferation Assay; Promega, Madison, WI). PC12 cells were seeded in a 96-well plate (6×10^3 cells/well) and maintained in culture for 48 h, changing medium after 24 h. The A42 peptide was added at a final concentration of 300 μM and incubated for 30 min at 37°C. At the end of this period, the CellTiter 96 AQ_{ueous} One Solution Reagent was added according to the manufacturer's instructions, and the plate was incubated in the dark for 2 h at 37°C. Absorbance was recorded at 490 nm using a Wallac 1420 multilabel counter (PerkinElmer Wallac, Boston, MA).

To obtain PC12 differentiation into sympathetic-like neurons, cells were seeded in eight-well poly(D-lysine)-coated culture slides (3000 cells/well) and cultured in the presence of 100 ng/ml fibroblast growth factor for 5 days. The culture medium containing fibroblast growth factor was replaced every 2 days. Before treatment with the fluorescein-labeled peptide, cells were rinsed twice with 8.1 mM Na_2HPO_4, 1.5 mM KH_2PO_4, pH 7.4, 136.8 mM NaCl, 2.7 mM KCl (PBS) containing 0.5 mM $MgCl_2$, and 0.6 mM $CaCl_2$ (Dulbecco's PBS) and then were incubated in serum-free F12K medium containing 1 mg/ml bovine serum albumin in the presence and absence of 100 μM fluorescent A42 peptide for 30 min, 3 h, and 6 h. At the end of the incubation times, cells were rinsed twice with Dulbecco's PBS and treated with the Image-iT-Live Plasma Membrane and Nuclear Labeling Kit (Molecular Probes, Carlsbad, CA) according to the manufacturer's instruction. Fluorescent specimens were viewed using a Zeiss Axioskop microscope (Carl Zeiss GmbH, Jena, Germany). Digital images were taken with a Leica DC100 camera (Leica, Wetzlar, Germany). The brightness and the contrast of the final images were adjusted using Adobe Photoshop version 6.00 (Adobe Systems, Mountain View, CA).

Peptide Synthesis. Peptides were synthesized manually, using a conventional solid-phase strategy based on the Fmoc/t-Bu protection chemistry. The crude products were purified to homogeneity by semi-preparative high-performance liquid chromatography. The final peptides were characterized by analytical high-performance liquid chromatography (purity, >98%) and mass spectrometry. Peptide sequences were as follows: H-Arg-Gln-Ile-Lys-Ile-Trp-Phe-Gln-Asn-Arg-Arg-Met-Lys-Trp-Lys-Lys for the carrier peptide (A40) and H-Arg-Gln-Ile-Lys-Ile-Trp-Phe-Gln-Asn-Arg-Arg-Met-Lys-Trp-Lys-

Lys-Arg-Val-Phe-Asn-Asp-Ala-Arg-Asp-Ile-Ile-Gln-Arg-Met-His-Leu-Arg-Gln-Tyr-Glu-Leu-Leu-OH (A42) for the membrane-permeable $G\alpha_s$ peptide (the $G\alpha_s$ C-terminal sequence is underlined). A fluorescent analog of A42 was prepared by EspiKem (Florence, Italy), linking carboxy-fluorescein to the peptide N terminus, spaced by a residue of ω-aminobutyric acid.

Peptides were dissolved in water to obtain 2 mM stock solutions. All peptide stock solutions were centrifuged at 11,000*g* for 4 min at room temperature, and supernatants were collected. The concentration of the membrane-permeable $G\alpha_s$ peptide was roughly estimated spectrophotometrically using the molar extinction coefficient for tyrosine at 280 nm (ϵ_{280nm} = 1400 $M^{-1} \cdot cm^{-1}$), as reported previously (Mazzoni et al., 2000).

Measurement of Intracellular cAMP. To study receptor-mediated cAMP accumulation, PC12 (passages 6–18) or HMEC-1 cells (passage 18–24) were seeded in 24-well culture plates at a density of approximately 6×10^4 or 1×10^5 cells/well and were used just after reaching confluence. Cells were preincubated in the presence of 100 μM papaverine with and without 1 U/ml of adenosine deaminase in F12K or MCDB 131 medium for 30 min at 37°C. Assays were initiated by the addition of 1 μM (PC12), 5 μM (HMEC-1) NECA, or 1 μM (HMEC-1) isoproterenol, followed by the incubation for 15 min at 37°C. Peptides (A40 or A42) were added 30 min before assay initiation, together with papaverine. At the end of the incubation time, the reaction was terminated by the removal of the reaction medium, followed immediately by the addition of 0.3 ml of 0.1 N HCl. The HCl extracts were collected into 15-ml Falcon tubes, and cells were rinsed with an additional 0.3 ml of 0.1 N HCl. Samples of the pooled HCl extract were centrifuged at 600*g* for 10 min. Aliquots (100 μl) of the supernatant were processed to measure cAMP content using the direct cAMP enzyme immunoassay kit from Sigma-Aldrich.

The effect of A42 on the concentration-response curve of NECA (0.1 nM to 5 μM) was evaluated by preincubating PC12 cells in the presence and absence of 10, 50, and 100 μM A42. The concentration-dependent effect of A42 was evaluated by preincubating PC12 cells with 11 different concentrations of the peptide ranging from 0.05 to 560 μM.

To study the effect of the membrane-permeable $G\alpha_s$ peptide on adenylyl cyclase and G_i signaling, PC12 cells were preincubated in the presence of 100 μM papaverine with and without 100 μM A42 in F12K medium for 30 min at 37°C. At the end of the preincubation period, either 10 μM forskolin, 1 μM ADPβS ($P2y_{12}$ receptor agonist), or both were added and incubated for 15 min at 37°C. Thereafter, the incubation medium was removed, 0.1 N HCl was added, and samples were processed as described above.

Measurement of Intracellular Calcium. Measurement of $[Ca^{2+}]_i$ was performed as described previously (Ceccarelli et al., 2003). In brief, confluent PC12 cells cultured in 24-well plates were incubated with and without 100 μM A42 in loading buffer (20 mM HEPES, pH 7.4, 130 mM NaCl, 5 mM KCl, 2 mM $CaCl_2$, 1 mM $MgSO_4$, 0.8 mM Na_2HPO_4, 0.2 mM NaH_2PO_4, 25 mM mannose, and 1 mg/ml bovine serum albumin) containing 2 μM Fluo-3 acetoxymethyl ester and 0.008% Pluronic F-127 for 30 min at 37°C. After incubation, cells were rinsed with detaching buffer (10 mM HEPES, pH 7.4, 140 mM NaCl, 5 mM KCl, 0.55 mM $MgCl_2$, and 3 mM EDTA) and incubated in the same buffer for 10 min at 37°C. Detached cells were harvested by low-speed centrifugation (1000*g*), resuspended in assay buffer (10 mM HEPES, pH 7.4, 140 mM NaCl, 5 mM KCl, 0.55 mM $MgCl_2$, and 1 mM $CaCl_2$), and analyzed on a FACScan flow cytometer with the CellQuest software (Becton Dickinson Labware; BD Biosciences, San Jose, CA).

To study receptor-mediated increase of $[Ca^{2+}]_i$, sample basal fluorescence was measured, and then 100 μM ATPγS ($P2y_2$ receptor agonist) was added. The cell flow was halted during this addition, and sample measurement was carried out within 2 to 3 s.

Data Analysis. Data from concentration-response curves were analyzed by a least-squares curve-fitting computer program (GraphPad Prism version 4.00 for Windows; GraphPad Software, San Diego, CA), and EC_{50} values were determined. Values represent the means ± S.E.M. of at least three independent experiments. The statistical significance of value differences was evaluated by the unpaired Student's *t* test using GraphPad Prism version 4.00.

NMR Spectroscopy. Samples for NMR spectroscopy were prepared by dissolving the appropriate amount of A42 in a water/SDS (SDS-d_{25}) solution, pH 6.6, to obtain concentrations of 2 mM peptide and 80 mM SDS-d_{25}. Dodecyl phosphocholine samples were prepared by dissolving the appropriate amount of A42 in water/dodecyl phosphocholine (DPC-d_{38}), pH 5.8, to obtain concentrations of 2 mM peptide and 15 mM DPC-d_{38}. NMR spectra were recorded on a Bruker DRX-600 spectrometer (Bruker, Newark, DE). One-dimensional NMR spectra were recorded in the Fourier mode with quadrature detection, and the water signal was suppressed by a low-power selective irradiation in the homogated mode. DQF-COSY (Piantini et al., 1982), TOCSY (Braunschweiler and Ernst, 1983; Bax and Davis, 1985), and NOESY (Jeener et al., 1979; Macura and Ernst, 1980) experiments were run in the phase-sensitive mode using quadrature detection in ω_1 by time-proportional phase increments of the initial pulse (Marion and Wühtrich, 1983).

Data block sizes comprised 2048 addresses in t2 and 512 equidistant t1 values. Before Fourier transformation, the time domain data matrices were multiplied by shifted sin2 functions in both dimensions. A mixing time of 70 ms was used for TOCSY experiments. NOESY experiments were run at 300 K, with mixing times in the range of 100 to 250 ms. The qualitative and quantitative analysis of DQF-COSY, TOCSY, and NOESY spectra were obtained using the SPARKY interactive program package (Goddard TD, Kneller DG, SPARKY 3, University of California, San Francisco, San Francisco, CA).

Spin-Label Experiments. NMR samples were prepared by dissolving A42 at a final concentration of 2 mM in 80 mM SDS solution dissolved in H_2O/D_2O. Assuming an SDS micelle aggregation number of 56, this corresponds to a micelle concentration of 1.8 mM. The H_2O/D_2O ratio was 90:10 (Lauterwein et al., 1979). The 5- and 16-doxyl stearic acids were solubilized in methanol-d_4 and then added to the samples.

Structure Calculation. Peak volumes were translated into upper distance bounds with the routine CALIBA of the DYANA software (Guntert et al., 1997). The necessary pseudoatom corrections were applied for nonstereospecifically assigned protons at prochiral centers and for the methyl group. After discarding redundant and duplicated constraints, the final list included 411 intraresidue and 125 inter-residue constraints, which were used to generate an ensemble of 200 structures by the standard protocol of simulated annealing in torsion angle space implemented in DYANA. No dihedral angle restraints and no hydrogen bond restraints were applied. The best 50 structures, which showed low values of the target functions (0.83–1.19) and small residual violations (maximum violation = 1.38 Å), were refined by in vacuo minimization using Discover module of MSI Insight II 2000 software, using cvff force field and applying a dielectric constant value of 1*r (MSI Molecular Simulations, San Diego, CA). First, the 50 structures were relaxed and then were constrained and unconstrained by using a combination of steepest descent and conjugate gradient minimization algorithms until the maximum RMS derivative was less than 0.01 kcal/Å. The resulting structures showed a root mean square deviation value of 0.9 Å on C atoms.

The minimum energy structure was subjected to a molecular dynamics procedure on peptide side chains, keeping the backbone geometry fixed. After an equilibration period of 10 ps, during which the temperature was gradually increased from 10 to 300 K, molecular dynamic simulations were run at 300 K for 600 ps. During molecular dynamics frame structures were saved each 10 fs. The final structures were analyzed using the Insight II 2000 program. Computations were performed on an Octane computer (SGI, Mountain View, CA).

Results

In a previous article, we reported that the α-helical conformation of $G\alpha_s$ C terminus is important to determine its ability to interact with the A_{2A} adenosine receptor, but this part of the $G\alpha_s$ molecule is not able to stabilize the high-affinity state of the receptor (Mazzoni et al., 2000; D'Ursi et al., 2002). Moreover, we have shown that a $G\alpha_s$ C-terminal 21-residue peptide $G\alpha_s(374–394)C^{379}A$ disrupts signal transduction and induces a conformational change of the receptor with stabilization of an intermediate affinity state for agonist ligands (Mazzoni et al., 2000). Now, we have designed and synthesized a 37-residue membrane-permeable peptide, A42, containing a 16-residue fragment (A40) derived from the homeodomain of the *D. melanogaster* transcription factor Antennapedia on the N-terminal side and $G\alpha_s(374–394)C^{379}A$ on the C-terminal side. A preliminary screening of cell-permeable peptide influence on PC12 cells demonstrated that preincubation of cell cultures with either 300 μM A40 or A42 peptide did not cause cell lysis (data not shown). The membrane-permeable $G\alpha_s$ peptide did not induce any reduction of cell viability, as shown by no variation of color development after the addition of the CellTiter 96 reagent between control (absorbance at 490 nm, 0.24 ± 0.02; $n = 4$) and peptide-treated (absorbance at 490 nm, 0.26 ± 0.01; $n = 4$) cells. The effects of A40 and A42 peptides on basal and adenosine receptor (A_{2A} and A_{2B} adenosine receptors)-stimulated cAMP accumulation in intact PC12 cells were evaluated. The addition of either one of the peptides had no significant effect on basal cAMP production (data not shown).

Analysis of A40 and A42 Effects on NECA-Stimulated cAMP Production in PC12 Cells. The effects of various concentrations of A40 or A42 on cAMP accumulation induced by stimulation with 1 μM NECA were measured in PC12 cells. The membrane-permeable $G\alpha_s$ peptide inhibited adenosine receptor-mediated cAMP production in a concentration-dependent manner, whereas the Antennapedia fragment had no major effect (Fig. 1). Analysis of data using a nonlinear curve-fitting program and statistical comparison of possible fits revealed that the A42 curve was better represented by a sigmoidal dose-response curve with variable slope than a simple sigmoidal dose-response curve ($p < 0.05$). The receptor-mediated cAMP production was completely inhibited at an A42 concentration of 560 μM, whereas the derived EC_{50} value was 5.30 ± 1.20 μM ($n = 4$).

To further characterize the mechanism sustaining A42 pharmacological activity, the effect of three different concentrations of the peptide on cAMP accumulation induced by PC12 stimulation with different concentrations of NECA was examined. Data obtained from stimulating cells with NECA in the absence of the peptide were analyzed and fitted using a nonlinear curve-fitting program (Fig. 2). Analysis revealed that the concentration-response curve was represented by a simple sigmoidal dose-response curve. The calculated EC_{50} value was 63.51 ± 10.50 nM ($n = 5$), whereas the maximal cAMP production was 296.81 ± 13.79 nM. Addition of 10, 50, or 100 μM A42 caused significant reductions of NECA efficacy (Fig. 2). In fact, at a NECA concentration of 1 μM, 10 and 50 μM A42 reduced agonist efficacy by 46 and 64%, respectively, compared with control values in the absence of A42 (Fig. 2). The concentration-response curves obtained in the presence of 10, 50, and 100 μM A42 were fitted by a simple sigmoidal dose-response model with EC_{50} values of 84.86 ± 29.60 ($n = 3$), 126.10 ± 28.20 ($n = 4$), and 104.90 ± 24.50 ($n = 3$) nM, respectively, indicating that the membrane-permeable $G\alpha_s$ peptide modulated agonist potency.

Analysis of A42 Specificity for Disrupting G_s-Coupled Receptors Signaling. To verify the specificity of the A42 effect at the interface between adenosine receptors and G_s, we examined whether the membrane-permeable $G\alpha_s$ peptide was able to directly inhibit adenylyl cyclase and/or disrupt $P2y_{12}$ and $P2y_2$ receptors coupling to G_i and G_q proteins, respectively. Both subtypes of P2y receptors are expressed in PC12 cells (Unterberger et al., 2002), and it is well established that $P2y_{12}$ activation leads to the inhibition of adenylyl cyclase, whereas $P2y_2$ activation induces an increase of $[Ca^{2+}]_i$ (Ralevic and Burnstock, 1998). The A42 peptide did not influence forskolin-induced cAMP in intact PC12 cells (Fig. 3), indicating that had no direct inhibitory effect on adenylyl cyclase. In addition, the peptide did not affect $P2y_{12}$ receptor-mediated inhibition of cAMP production (Fig. 3).

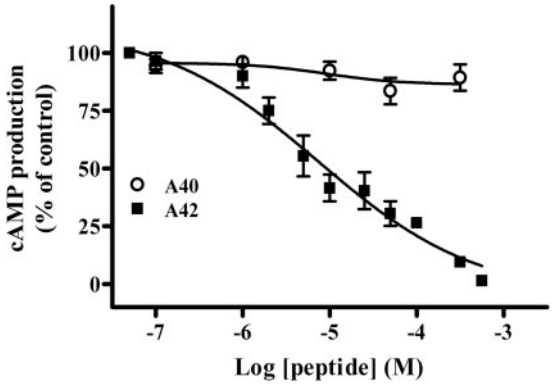

Fig. 1. Concentration-dependent effect of A40 and A42 peptides on NECA-stimulated cAMP production in PC12 cells. PC12 cells were incubated with various concentrations of either A40 or A42 in the presence of 1 μM NECA as described under *Materials and Methods*. Control value in the absence of peptides was 304.12 ± 15.09 nM cAMP ($n = 5$). Values are the mean ± S.E.M. of three (A40) and five (A42) independent experiments each performed in duplicate. The EC_{50} value was determined by fitting data as a sigmoidal dose-response curve with variable slope using GraphPad Prism version 4.00.

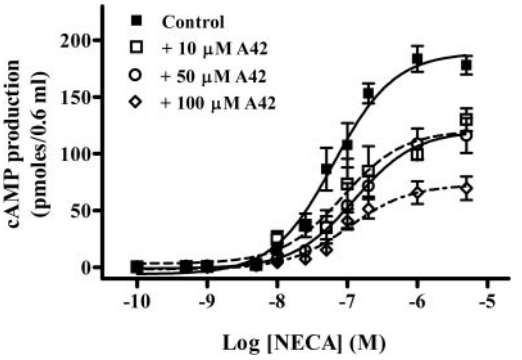

Fig. 2. Modulation of NECA-stimulated cAMP production by the A42 peptide in PC12 cells. PC12 cells were incubated with different concentrations of NECA in the presence and absence of 10, 50, or 100 μM A42. Accumulation of cAMP was determined as described under *Materials and Methods*. In the absence of both NECA and A42, basal value of cAMP accumulation was 1.10 ± 0.40 nM ($n = 5$), whereas in the presence of 10, 50, and 100 μM A42, basal values were 0.70 ± 0.14 ($n = 3$), 1.02 ± 0.22 ($n = 4$), and 1.41 ± 0.10 ($n = 3$) nM. Values are the mean ± S.E.M. of three to five independent experiments each performed in duplicate. The EC_{50} values were determined by fitting data as sigmoidal dose-response curves using the GraphPad Prism version 4.00 computer program.

Stimulation of P2y2 receptors with 100 μM ATPγS induced a 2-fold increase of $[Ca^{2+}]_i$ in PC12 (Fig. 4), which was not modulated by the addition of A42. These results indicate that the membrane-permeable $G\alpha_s$ peptide did not influence the interactions between P2y receptors and G_i/G_q proteins supporting the specificity of peptide activity.

The ability of A42 to inhibit receptor-mediated cAMP production was also evaluated in HMEC-1, a human microvascular endothelial cell line, which constitutively expresses both A_{2A} and A_{2B} adenosine receptors (Feoktistov et al., 2002) and β-adrenergic receptors (Gornikiewicz et al., 2000). In this cell line, A_{2B}/A_{2A} mRNA ratio is approximately 4:1 (Feoktistov et al., 2002), whereas in PC12 cells, although both A_{2A} and A_{2B} mRNA were expressed (Arslan et al., 1999), the A_{2A} adenosine receptor seems to be the major adenosine receptor subtype involved in NECA-stimulated effector activation in some cellular clones (Arslan et al., 1999). Indeed, HMEC-1 stimulation with 5 μM NECA induced a cAMP production of 102.07 $\pm$ 12.44 nM, whereas in PC12 cells, stimulation with the same concentration of NECA caused a cAMP production of 296.80 $\pm$ 13.79 nM. The A42 peptide significantly inhibited NECA-stimulated cAMP production in HMEC-1, although the control peptide (A40) had no major inhibitory effect (Fig. 5). In addition, A42 inhibited β-adrenergic receptor-mediated cAMP production, even though 1 μM isoproterenol caused a moderate accumulation of cAMP (51.63 $\pm$ 10.84 nM) in HMEC-1.

Analysis of Fluorescent A42 Peptide Internalization. To verify the ability of the A42 peptide to cross cell membranes, we synthesized a carboxy-fluorescein-labeled derivative of such peptide and incubated neuronal differentiated PC12 cells in the presence and absence of a fixed concentration of such fluorescent peptide for various times. Neuronal-differentiated PC12 cells were preferred over undifferentiated cells because the distribution of the fluorescent membrane-permeable peptide along the neurites can be analyzed. Living cells were labeled with the fluorescent peptide followed by membrane staining with the Image-iTLive Plasma Membrane and Nuclear Labeling Kit. In Fig. 6, digital images of fluorescent cells are shown. Figure 6, A and B, illustrates cell labeling with the fluorescein-conjugated A42 peptide (green fluorescence) after 30 min and 3 h of incubation, respectively. At 30 min, the fluorescent peptide was localized on plasma membrane in both cell bodies and neurites, whereas after 3 and 6 h (data not shown), the fluores-

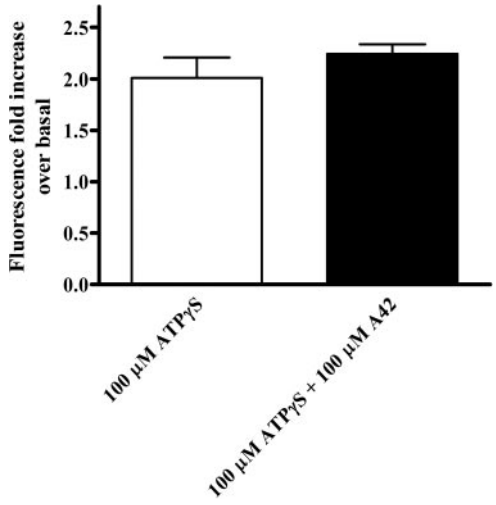

Fig. 4. The A42 peptide does not affect $P2y_2$-mediated increase of $[Ca^{2+}]_i$ in PC12 cells. Confluent PC12 cells cultured in 24-well plates were incubated with and without 100 μM A42 in a loading buffer containing 2 μM Fluo-3 acetoxymethyl ester and 0.008% Pluronic F-127 for 30 min at 37°C. Cells were detached, harvested, and analyzed on a FACScan flow cytometer as described under *Materials and Methods*. The basal fluorescence was recorded for each sample, and then the agonist (100 μM ATPγS) was added. The basal $[Ca^{2+}]_i$ was determined as described previously (Ceccarelli et al., 2003). Values are the mean $\pm$ S.E.M. of three independent experiments each performed in duplicate.

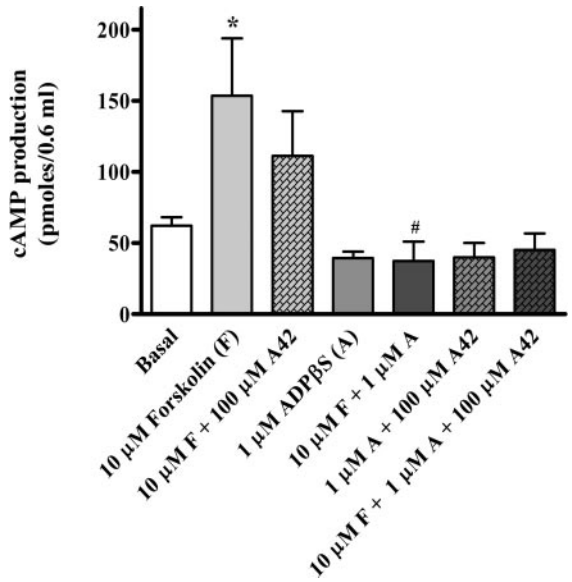

Fig. 3. The A42 peptide does not directly modulate adenylyl cyclase and $P2y_{12}$ receptor signaling to G_i. PC12 cells were preincubated in the presence and absence of 10 μM forskolin with and without 100 μM A42 for 30 min at 37°C. Then, some samples were stimulated with 1 μM ADPβS. Accumulation of cAMP was determined as described under *Materials and Methods*. Values are the mean $\pm$ S.E.M. of three independent experiments each performed in duplicate. Values that are significantly different from either basal (*, $p < 0.05$) or forskolin-stimulated (#, $p < 0.05$) value as determined by unpaired Student's t test are indicated.

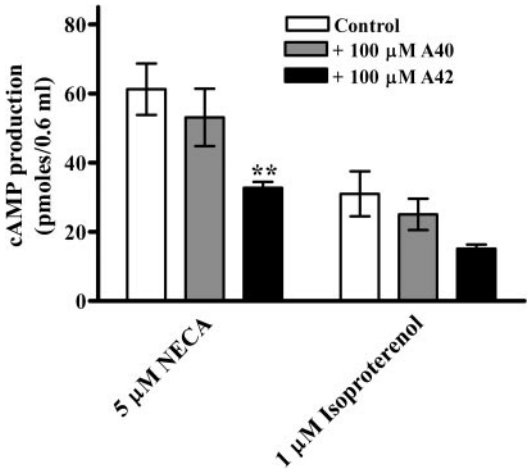

Fig. 5. Inhibition of NECA- and isoproterenol-stimulated cAMP production by the A42 peptide in HMEC-1. Confluent HMEC-1 cultured in 24-well plates were incubated with and without 100 μM A42 in complete MCDB 131 medium containing 100 μM papaverine for 30 min at 37°C. Then, either 5 μM NECA or 1 μM isoproterenol was added to appropriate wells. Accumulation of cAMP was determined as described under *Materials and Methods*. Values are the mean $\pm$ S.E.M. of three independent experiments each performed in duplicate. Value that are significantly different from control value (**, $p < 0.01$) as determined by unpaired Student's t test are indicated.

cent staining was detectable inside cells. The fluorescein (green fluorescence) staining overlapped the Alexa Fluor 594 wheat germ agglutinin (red fluorescence) staining on plasma membranes (Fig. 6, C and D).

NMR Spectroscopy. The membrane environment for NMR studies is usually mimicked by surfactant supramolecular aggregates, generally constituted by an apolar inner core and a hydrophilic exposed interface. Although a variety of surfactant supramolecular structures have been proposed for NMR analysis, the choice is limited because of the high costs of the surfactant deuteration and usually low quality of spectra produced in such systems. Micellar solutions of SDS, DPC, and dipalmitoyl phosphatidyl cholin are typically used for NMR investigations (Bader et al., 2003).

A whole set of one- and two-dimensional protonic spectra were recorded in aqueous solution of 80 mM SDS and 15 mM DPC solution. To check the absence of peptide aggregation states, spectra were acquired within the concentration range of 0.5 to 15 mM. No significant changes were observed in the distribution and shape of the ^{1}H resonances, indicating that no aggregation phenomena occurred within this concentration range.

Because of the better quality of SDS NMR spectra versus DPC NMR spectra, the complete resonance assignments of A42 were achieved in SDS micellar solution according to the method of Wüthrich (1986) via the usual systematic application of DQF-COSY (Piantini et al., 1982), TOCSY (Braunschweiler and Ernst, 1983; Bax and Davis, 1985), and NOESY (Jeener et al., 1979; Macura and Ernst, 1980) experiments with the support of SPARKY software package. The resonances of several CHα were shifted up-field, suggesting the involvement of these residues in α-helix or in-turn secondary structure (Wishart et al., 1991).

The pattern of NOE connectivities observed in NOESY spectra (data not shown) were consistent with the presence of two helical stretches localized at N and C termini of the A42 peptide. In Figs. 7 and 8, the N- and C-terminal helices are represented with violet and cyan ribbons, respectively. Low regularity in the dihedral angle patterns was detectable at the level of residues 11 to 17.

Structure Calculation. Three-dimensional structures of A42 were calculated by simulated annealing in torsion angle space and restrained molecular dynamics methods based on 536 NOE-derived restraints using DYANA software package (Guntert et al., 1997). Among 200 calculated structures, the resulting best 50 ones were selected according to the lowest

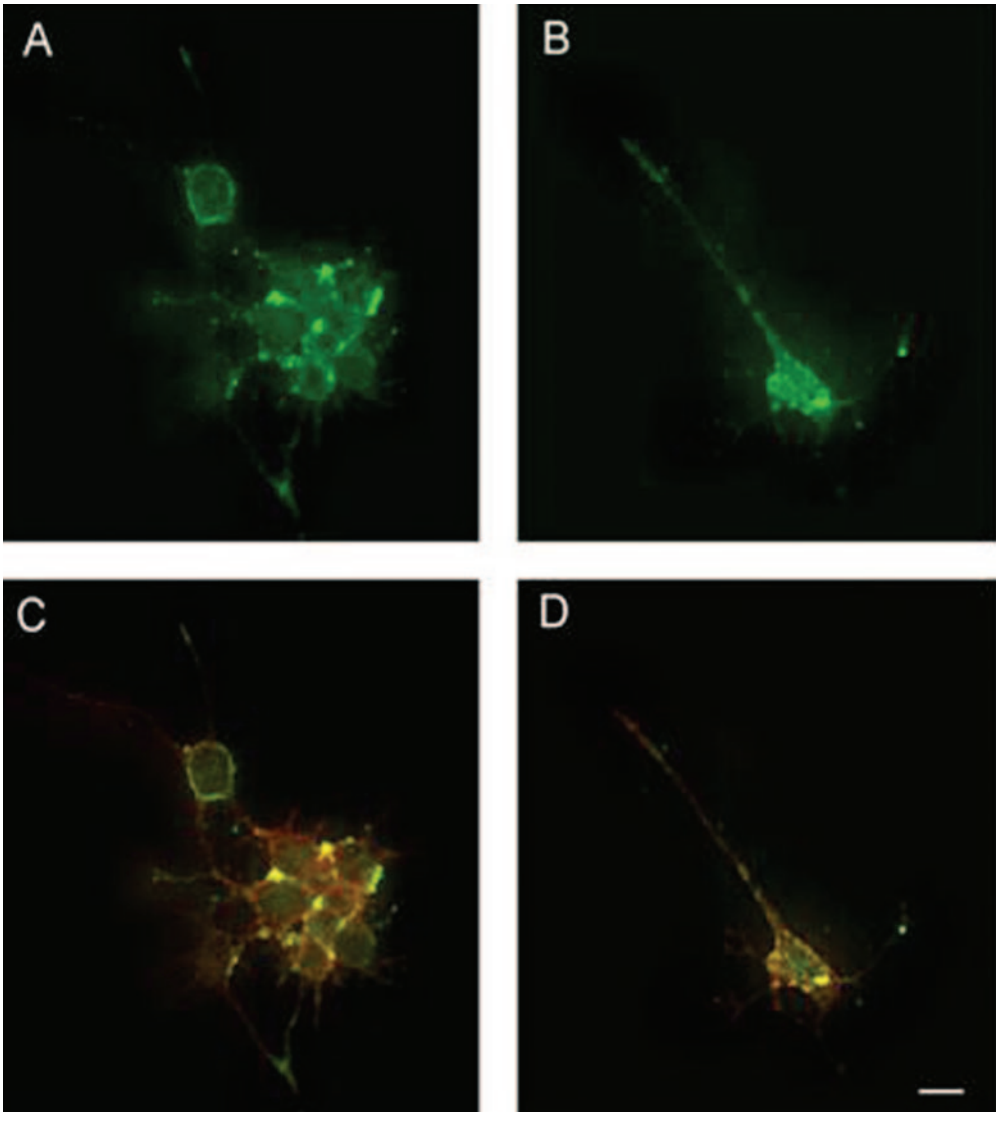

Fig. 6. Fluorescence photomicrographs of neuronal differentiated PC12 live cells. In A and C, cells were incubated with the fluorescent peptide for 30 min, whereas in B and D, for 3 h. In C and D, cells were stained with Image-iT Live Kit labeling plasma membranes with Alexa Fluor 594 wheat germ agglutinin (red fluorescent). Scale bar, 20 μm.

values of their target function. They were subjected to further procedures of minimization by Discover module of Insight II (MSI Molecular Simulations) using the DYANA derived restraints with a force constant value of 1. The inspection of the torsion angles according to the PROCHECK (Laskowski et al., 1996) software pointed out, for most of the calculated structures, the presence of two separate helical regions including residues 3 to 10 and 18 to 35. In Table 1, the statistic of the structure calculation is reported.

Spin-Label Studies. The positioning of the peptide relative to the surface and interior of the SDS micelle was studied using the paramagnetic probes 5- and 16-doxyl stearic acids. Both compounds contain doxyl head groups, a cyclic nitroxide with unpaired electron, which is bound to the aliphatic chain carbon in position 5 or 16, respectively. These paramagnetic probes are expected to cause broadening of the NMR signals and decrease of resonance intensities from residues inside but close to the surface (5-doxyl) or deeply buried in the micelle (16-doxyl), respectively (Jarvet et al., 1997; Lindberg et al., 2001).

TOCSY spectra of A42 in the presence and absence of the spin labels were recorded, keeping constant all other conditions. Just a few residues were affected by the presence of 5-doxylstearic acid. Particularly, Asp^{21} and Met^{29} NH/α signals nearly disappeared. On the other hand, the A42 spectrum, acquired in the presence of 16-doxyl stearic acid, evi-

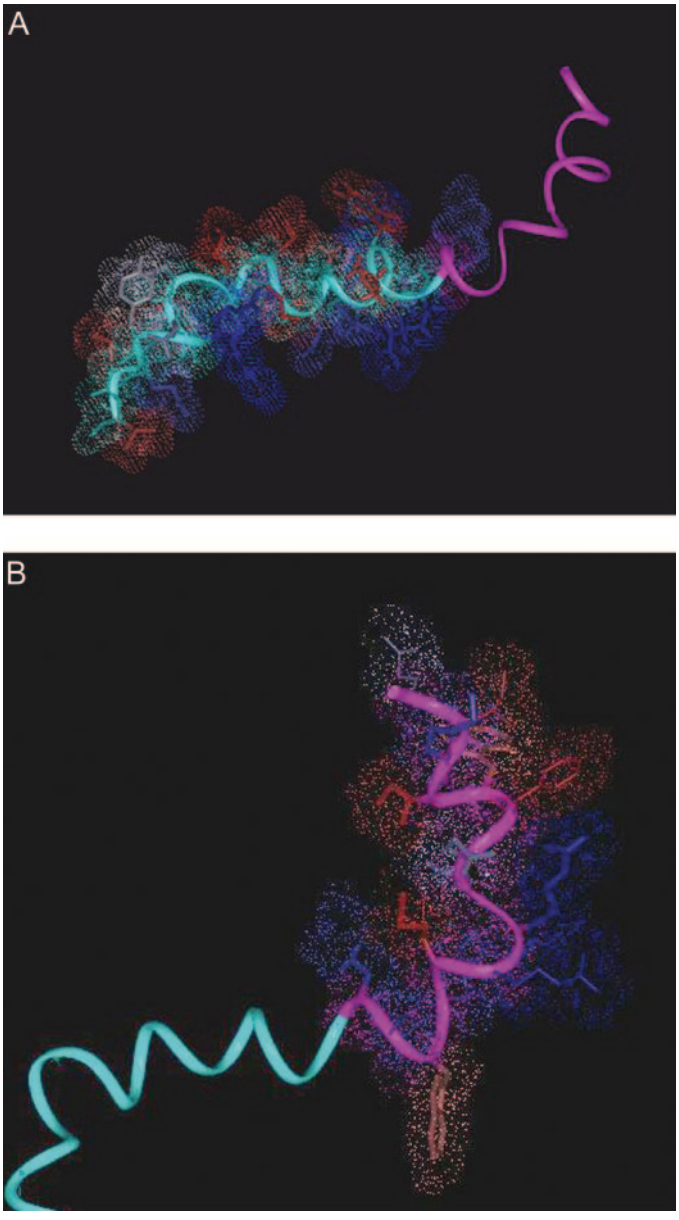

Fig. 7. NMR structure of A42 in SDS micellar solution (600 Mhz, 300 K, mixing time 150 ms). The helical stretches are outlined by violet (penetratin) and cyan ($G\alpha_s$) ribbons. The electrostatic surfaces of 18 to 36 (A) and 3 to 10 α-helices (B) are displayed. A, electrostatic surface of the 18 to 36 region of A42. Polar region (colored in blue) is lined by residues corresponding to Asp^{21}, Arg^{23}, Asp^{24}, and Arg^{28}. Two hydrophobic planes (colored in red) are defined by less polar residues Ile^{25}, Ile^{26}, Met^{29}, His^{30}, Tyr^{34}, and Leu^{36}. B, electrostatic surface of the 3 to 10 α-helical fragment. The side chains defining clusters of hydrophobic (tryptophan) and hydrophilic residues are displayed and colored according to their hydrophobicity.

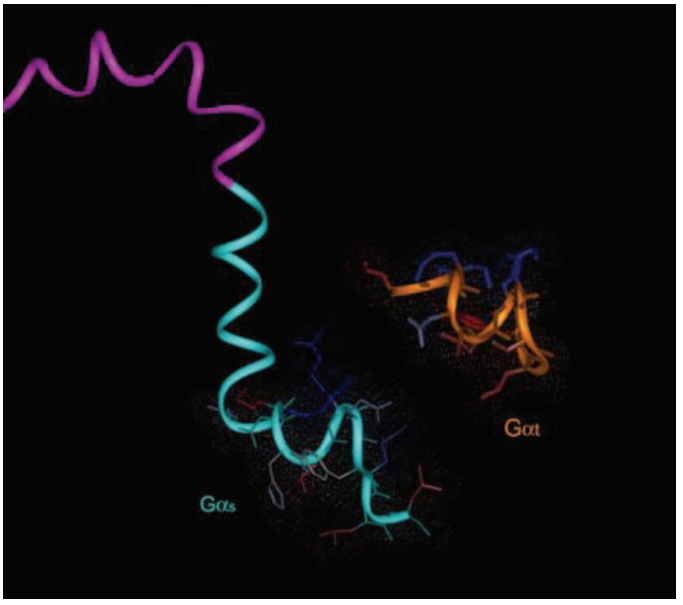

Fig. 8. Comparison of the conformational properties of the last 11 C-terminal residues of A42 (NMR structure in micellar solution) (blue) and the corresponding region of $G\alpha_t$ derived from Koenig's model (orange) (Koenig et al., 2002). The side chains of fragments are displayed and colored according to their hydrophobicity.

TABLE 1
Statistical information for A42 structure calculation

Distant restraints	
Total	536
Intra-monomer	411
Inter-monomer	125
Sequential (i − j = 1)	78
Medium (i − j = 2, 3, 4)	47
RMSD analysis	
Ile^3-Arg^{10} backbone	0.83 ± 0.30Å
Ile^3-Arg^{10} heavy atoms	1.75 ± 0.43Å
Asn^{20}-Tyr^{34} backbone	0.96 ± 0.48Å
Asn^{20}-Tyr^{34} heavy atoms	1.85 ± 0.60Å
NOEs violations >0.1 Å	
Total violations	7
Highest	0.27
Lowest	0.12
Average violation	0.17 ± 0.05Å
Average energy (kcal/mol)	
Total energy	600 ± 5
Bond energy	120 ± 1
Phi energy	28 ± 3
Theta energy	235 ± 7
Out of plane energy	0.91 ± 0.03
Nonbonded energy	217 ± 12

denced that Arg[1], Gln[2], Ile[3], Phe[7], Arg[11], Lys[13], Lys[15], Val[18], Phe[19], Ala[22], Arg[23], Ile[25], Met[29], Leu[36], and Leu[37] were drastically affected by 16-doxylstearic acid, with a nearly disappearing of NH/α signals. These results provided strong evidences that A42 had a significant preference to be deeply buried in the micelles.

Discussion

The increasing knowledge of disease molecular basis has prompted the development of new classes of specific drugs such as peptide/polypeptide- or DNA-based drugs. Unfortunately, often these biomolecules show limited ability to cross the plasma membrane, resulting in poor cellular access, which largely prohibits them from reaching intracellular targets.

We developed previously a $G\alpha_s$ 21-residue synthetic peptide that inhibits A_{2A} adenosine receptor-mediated activation of adenylyl cyclase in rat striatal membranes (Mazzoni et al., 2000). Here, we created a cell-permeating version of such peptide by N-terminal modification with the cell-permeation sequence (16 residues) from the homeodomain of Antennapedia. Besides studying the biological activity and intracellular transfer of the cell-permeable $G\alpha_s$ peptide, its structural properties were analyzed by NMR. This part of the work was a necessary step to confirm the ability of the $G\alpha_s$ segment to acquire an α-helical conformation (Mazzoni et al., 2000), even in the contest of a chimeric peptide. The α-helix structure of the 21-residue $G\alpha_s$ peptide overlaps that of the $G\alpha_s$ C terminus, shown by the crystal structure resolution (Sunahara et al., 1997), and is pivotal for its biological activity (Mazzoni et al., 2000). In addition, structural studies of the chimeric peptide in a membrane-mimicking environment are useful to elucidate the mechanism of penetratin internalization, an issue which is still debated (Richard et al., 2003).

The Membrane-Permeable $G\alpha_s$ Peptide Is an Inhibitor of Receptor-Stimulated cAMP Production in PC12 Cells and HMEC-1. The membrane-permeable $G\alpha_s$ peptide (A42) did not affect cell viability but significantly inhibited adenosine receptor-mediated cAMP accumulation in PC12 cells, whereas the permeation sequence (A40) did not show any effect. These results prompted us to investigate the pharmacological profile of this inhibition by studying the concentration-dependent effect of the peptide. The A42 peptide was a potent inhibitor of cAMP accumulation in PC12 cells with an EC_{50} value of approximately 5 μM. The membrane-permeable peptide caused a dramatic decrease of agonist maximal efficacy. This effect was evident at a peptide concentration close to its EC_{50} value. At higher peptide concentrations, NECA potency was also modulated. The observed reduction of NECA efficacy suggests that A42 competes with $G\alpha_s$ for interaction with adenosine receptor, leading to a decreased number of activated $G\alpha_s$. The molecular basis supporting the decrease of NECA potency is less evident, but a shift of receptor affinity state for agonist ligands may be involved, as suggested by our previous observations (Mazzoni et al., 2000). In contrast, to direct $G\alpha$ protein inhibitors such as suramin and analogs (Freissmuth et al., 1999), the inhibition caused by A42 seems to be mixed competitive. Whereas suramin acts with several mechanisms in preventing receptor-mediated G protein activation, including suppression of spontaneous GDP-release from $G\alpha$ subunits and competition with receptors for binding to G proteins (Freissmuth et al., 1999), our membrane-permeable $G\alpha_s$ peptide does not directly modulate GDP/GTP exchange, but it competes with $G\alpha_s$ for interacting with receptors. Thus, A42 decreasing the number of productive receptor G_s interactions causes a reduction of agonist efficacy, whereas its binding to the receptor induces a decrease of receptor affinity for the agonist, which seems as reduction of agonist potency.

The A42 peptide did not directly modulate adenylyl cyclase activity and did not affect G_i- and G_q-coupled receptor signaling. Such observations are indicative that the specific peptide target is the receptor G_s interface. Sequence alignment of $G\alpha_s$, $G\alpha_i$, and $G\alpha_q$ C termini shows that the differences are restricted to a few key regions. However, these key residues are the structural determinants of receptor $G\alpha$ specificity of interaction (Cabrera-Vera et al., 2003). Our 21-residue $G\alpha_s$ peptide was chosen on the basis of its ability to inhibit A_{2A} adenosine receptor-mediated production of cAMP in rat striatal membranes (Mazzoni et al., 2000), whereas an 11-residue peptide was less effective. However, we must point out that because the A_{2A} adenosine receptor in rat striatum is coupled to G_{olf} (Corvol et al., 2001), we may have directed our selection toward a tool effective in disrupting their interaction. On the other hand, G_{olf} shares extensive amino acid identity with $G\alpha_s$ (Jones and Reed, 1989), and divergences are not localized in the extreme C-terminal region. Others (Feldman et al., 2002) have shown that an 83-residue polypeptide derived from the C terminus of $G\alpha_s$ specifically inhibits G_s signaling in human embryonic kidney 293 cells. The A42 peptide was able to inhibit adenosine and β-adrenergic receptor-mediated cAMP production in a human cell line (HMEC-1), although with a lower effectiveness than in PC12 cells. This observation may indicate a certain selectivity of the peptide for inhibiting A_{2A} adenosine receptor coupling to G_s proteins or may result as a consequence of the different ability of A42 to penetrate human endothelial cell plasma membrane.

The use of the carboxy-fluorescein-labeled A42 peptide proved to be a very effective strategy to verify peptide translocation inside of differentiated PC12 cells. Within 30 min, the A42 peptide is localized exclusively on plasma membrane, whereas later (3–6 h) is distributed between plasma membrane and cytoplasm. These results are particularly relevant because they are obtained in live cells and correlate the peptide localization on plasma membrane with its ability to inhibit adenosine receptor-mediated activation of the G_s protein.

The use of membrane-permeable peptides to disrupt protein/protein interfaces and thus manipulate intracellular signaling pathways has attracted the interest of numerous investigators. Various peptides (cargo) have been successfully delivered inside cells through their conjugation to cell-penetrating peptides (carrier) such as pentratin (43–58) and transactivating regulatory protein (49–57) (Eiden, 2005).

Two types of approaches have been used in the past to inhibit signaling from G_s-coupled receptors in intact cells. Chang et al. (2000) successfully created a membrane-permeable $G\alpha_s$ peptide by fusing with a chemical reaction the Kaposi fibroblast growth factor signal sequence to the N terminus of $G\alpha_s$, the last 11-residue fragment. On the other hand, Feldman et al. (2002) selectively inhibited G_s signaling in human embryonic kidney 293 cells by transfection with a

minigene encoding for a 83-residue polypeptide derived from the C terminus of $G\alpha_s$. Both approaches have produced interesting and useful results but also present some inconveniences that need improvement. In the case of the Kaposi fibroblast growth factor signal sequence-fused peptide, the $G\alpha_s$ C-terminal sequence is rather short, and the membrane-permeable peptide is obtained by using chemical oxidation followed by conjugation. The whole A42 peptide was synthesized by the conventional solid-phase strategy. On the other hand, the minigene approach cannot be suitable for all cell types.

NMR Analysis Reveals the α-Helical Conformation and Preference for a Hydrophobic Environment of the Membrane-Permeable $G\alpha_s$ Peptide. Structural data support the interpretation of biological observations in the key of significant biomolecular interactions. Therefore, we undertook a full NMR investigation of the A42 peptide in membrane-mimetic environments to compare its structure with that of the 21-residue $G\alpha_s$ peptide described previously (Mazzoni et al., 2000). The choice of the membrane-like solvent was motivated on the fact that both the penetratin and the $G\alpha_s$ segments are involved in membrane interactions.

NMR spectra were record in SDS and DPC micellar solutions, but data of the best quality were obtained in SDS micellar solutions. At a greater concentration than its critical micellar concentration (8 mM at 25°C), NMR experiments showed that A42 was arranged in two stretches of α-helical structure encompassing, respectively, residues 3 to 10 and 18 to 36. It is noticeable that even in a membrane-mimicking environment and in conjugation with a cell-penetrating peptide, the segment 18 to 36 can be well overlapped with the previously solved structure of the corresponding $G\alpha_s(374–394)C^{379}A$ peptide (D'Ursi et al., 2002) and even with the crystal structure of the $G\alpha_s$ protein (Sunahara et al., 1997). This demonstrates that the presence of the penetratin segment does not affect the conformational stability and functionality of the $G\alpha_s(374–394)C^{379}A$ peptide.

The inspection of the electrostatic surface showed that the helix 18 to 36 was amphipathic (Fig. 7) with the presence of a polar surface lined by Asp^{378}, Arg^{380}, Asp^{381}, and Arg^{385} and two hydrophobic surfaces defined by less polar residues Ile^{382}, Ile^{383}, Met^{386}, His^{387}, Tyr^{391}, and Leu^{393}. The analysis of the side-chain assessment and the comparison with the $G\alpha_s(374–394)C^{379}A$ structure highlighted that Asp^{378}, Asp^{381}, Ile^{383}, and Leu^{388} were in a significantly ordered conformation (Fig. 7A). Several studies attribute an important role to these amino acids as highly conserved residues directly involved in G protein receptor interaction (Kisselev et al., 1998). In particular, it has been demonstrated by numerous biological evidences that a constant of the GPCR/G protein coupling is an electrostatic interaction involving highly conserved aspartic acid residues of Gα C-terminal region with the highly conserved DRY motif of the receptors (Kisselev et al., 1998). These contacts seem to be stabilized by multihelix interaction with C-terminal residues of the receptor involving several conserved hydrophobic residues such as Ile^{383} and Leu^{388}.

It is interesting that the arrangement of the side chains of the 18 to 36 helix in A42, in particular those residues retained as important for the interaction with the cognate receptor (Kisselev et al., 1998), was comparable with the orientation observed in the C-terminal $G\alpha_t$ undecapeptide structure derived from the model of the G protein/receptor complex proposed by Koenig et al. (2002) (Fig. 8). Thus, a consistency was evident between the models of the C-terminal Gα helix, in the whole receptor/G protein complex and those of its related $G\alpha_s(374–394)C^{379}A$ peptide, even conjugated with a delivery molecule. There are sufficient data to believe that the conservation of these fundamental structural characters is responsible for the activity of the C-terminal peptide as that of the whole $G\alpha_s$ protein.

TOCSY experiments of A42 in micelle solution, acquired alternatively, in the presence of 5- and 16-doxyl stearic acids, showed that the peptide was generally more sensitive to the action of 16-doxyl stearic acid, the inner core probe of the micelle. In particular, among the residues affected by 16-doxyl-stearic acid, four residues belonged to the C-terminal penetratin portion. These data supported the structural determinant of the penetratin delivery ability and showed that the conjugation of the penetratin peptide with a cargo did not affect the modality of its delivery functionality.

The distribution of the molecular surface of the penetratin segment compared with the $G\alpha_s(374–394)C^{379}A$ portion in A42 allows the formulation of a hypothesis on how the fine arrangement of the side chains can be related to the functionality of the biomolecule. Whereas the distribution of polar and hydrophobic residues defined an amphipathic α-helix in the $G\alpha_s(374–394)C^{379}A$ region, which seemed tailored to allow peptide key interactions with receptors, in the penetratin region, the distribution of the side chains is in such way to form clusters of hydrophobic and hydrophilic surfaces at the N terminus and in the center of the fragment, respectively (Fig. 7B). The clustering of hydrophobic and hydrophilic residues is consistent with the most recent hypotheses, which re-establish the role of endocytosis in the internalization of cationic CPP (Richard et al., 2003). The effect of the spin labels causes speculation on the A42 segment boundary that is inserted in the core of the micelle. In fact, the experiments in the presence of 5-doxyl stearic acid showed that only a few residues were localized in proximity of the micelle surface. In particular, residues 19 and 20 corresponding to the N-terminal region of the $G\alpha_s(374–394)C^{379}A$ portion were those significantly sensitive to the action of the surface probe of the micelle so that in a transport process, they can define the boundary between the region inserted in the membrane and that exposed on the surface.

In conclusion, our biological data, in conjugation with conformational analysis and fluorescence microscopy studies, indicate that the A42 peptide is a valuable, nontoxic research tool for modulating G_s-coupled receptor signal transduction. These results represent the starting point for the development of new peptomimetic drug candidates acting at the intracellular level.

Acknowledgments

We are grateful to A. Asta for expert technical assistance.

References

Arslan G, Kull B, and Fredholm BB (1999) Signaling via A_{2A} adenosine receptor in four PC12 cell clones. *Naunyn-Schmiedeberg's Arch Pharmacol* **359:**28–32.

Bader R, Lerch M, and Zerbe O (2003) NMR of membrane-associated peptides and proteins, in *Methods and Principles in Medicinal Chemistry: BioNMR in Drug Research,* vol 16, pp 95–120, Wiley, Weinheim.

Bax A and Davis DG (1985) Mlev-17-based two-dimensional homonuclear magnetization transfer spectroscopy. *J Magn Reson* **65:**355–360.

Braunschweiler L and Ernst RR (1983) Coherence transfer by isotropic mixing: application to proton correlation spectroscopy. *J Magn Reson* **53:**521–528.
Cabrera-Vera TM, Vanhauwe J, Thomas TO, Medkova M, Preininger A, Mazzoni MR, and Hamm HE (2003) Insights into G protein structure, function and regulation. *Endocr Rev* **24:**765–781.
Ceccarelli F, Scavuzzo MC, Giusti L, Bigini G, Costa B, Carnicelli V, Zucchi R, Lucacchini A, and Mazzoni MR (2003) ET_A receptor-mediated Ca^{2+} mobilisation in H9c2 cardiac cells. *Biochem Pharmacol* **65:**783–793.
Chang M, Zhang L, Tam JP, and Sanders-Bush E (2000) Dissecting G protein-coupled receptor signaling pathways with membrane-permeable blocking peptides. Endogenous 5-HT_{2C} receptors in choroid plexus epithelial cells. *J Biol Chem* **275:**7021–7029.
Corvol JC, Studler JM, Schonn JS, Girault JA, and Herve D (2001) $G\alpha_{olf}$ is necessary for coupling D1 and A2a receptors to adenylyl cyclase in the striatum. *J Neurochem* **76:**1585–1588.
Derossi D, Joliot AH, Chassaing G, and Prochiantz A (1994) The third helix of the Antennapedia homeodomain translocates through biological membranes. *J Biol Chem* **269:**10444–10450.
D'Ursi AM, Albrizio S, Greco G, Mazzeo S, Mazzoni MR, Novellino E, and Rovero P (2002) Conformational analysis of the Gα protein C-terminal portion. *J Pept Sci* **8:**576–588.
Eiden LE (2005) Fusion polypeptides that inhibit exocytosis: fusing aptamer and cell-penetrating peptide technologies and pharmacologies. *Mol Pharmacol* **67:** 980–982.
Feldman DS, Zamah AM, Pierce KL, Miller WE, Kelly F, Rapacciuolo A, Rockman HA, Koch WJ, and Luttrell LM (2002) Selective inhibition of heterotrimeric Gs signaling. Targeting the receptor-G protein interface using a peptide minigene encoding the $G\alpha_s$ carboxyl terminus. *J Biol Chem* **277:**28631–28640.
Feoktistov I, Goldstein AE, Ryzhov S, Zeng D, Belardinelli L, Voyno-Yasenetskaya T, and Biaggioni I (2002) Differential expression of adenosine receptors in human endothelial cells: role of A_{2B} receptors in angiogenic factor regulation. *Circ Res* **90:**531–538.
Freissmuth M, Waldhoer M, Bofill-Cardona E, and Nanoff C (1999) G protein antagonists. *Trends Pharmacol Sci* **20:**237–245.
Gilchrist A, Bunemann M, Li A, Hosey MM, and Hamm HE (1999) A dominant-negative strategy for studying roles of G proteins in vivo. *J Biol Chem* **274:**6610–6616.
Gornikiewicz A, Sautner T, Brostjan C, Schmierer B, Fugger R, Roth E, Muhlbacher F, and Bergmann M (2000) Catecholamines up-regulate lipopolysaccharide-induced IL-6 production in human microvascular endothelial cells. *FASEB J* **14:**1093–1100.
Guntert P, Mumenthaler C, and Wüthrich K (1997) Torsion angle dynamics for NMR structure calculation with the new program DYANA. *J Mol Biol* **273:**283–298.
Havlickova M, Blahos J, Brabet I, Liu J, Hruskova B, Prezeau L, and Pin JP (2003) The second intracellular loop of metabotropic glutamate receptors recognizes C termini of G-protein α-subunits. *J Biol Chem* **278:**35063–35070.
Jarvet J, Zdunek J, Damberg P, and Graslund A (1997) Three-dimensional structure and position of porcine motilin in sodium dodecyl sulfate micelles determined by 1H NMR. *Biochemistry* **36:**8153–8163.
Jeener J, Meyer BH, Bachman P, and Ernst RR (1979) Investigation of exchange processes by two-dimensional NMR spectroscopy. *J Chem Phys* **71:**4546–4553.
Jones DT and Reed RR (1989) Golf: an olfactory neuron specific-G protein involved in odorant signal transduction. *Science (Wash DC)* **244:**790–795.
Kisselev OG, Kao J, Ponder JW, Fann YC, Gautam N, and Marshall GR (1998) Light-activated rhodopsin induces structural binding motif in G protein α-subunit. *Proc Natl Acad Sci USA* **95:**4270–4275.
Kobilka BK, Kobilka TS, Daniel K, Regan JW, Caron MG, and Lefkowitz RJ (1988) Chimeric α2-, β2-adrenergic receptors: delineation of domains involved in effector coupling and ligand binding specificity. *Science (Wash DC)* **240:**1310–1316.
Koenig BW, Kontaxis G, Mitchell DC, Louis JM, Litman BJ, and Bax A (2002) Structure and orientation of a G protein fragment in the receptor bound state from residual dipolar couplings. *J Mol Biol* **322:**441–461.
Kostenis E, Conklin BR, and Wess J (1997) Molecular basis of receptor/G protein coupling selectivity studied by coexpression of wild type and mutant m_2 muscarinic receptors with mutant $G\alpha_q$ subunits. *Biochemistry* **36:**1487–1495.
Laskowski RA, Rullmannn JA, MacArthur MW, Kaptein R, and Thornton JM (1996) AQUA and PROCHECK-NMR: programs for checking the quality of protein structures solved by NMR. *J Biomol NMR* **8:**477–486.
Lauterwein J, Bosch C, Brown LR, and Wüthrich K (1979) Physiochemical studies of the protein-lipid interactions in melittin containing micelles. *Biochim Biophys Acta* **556:**244–264.
Lindberg M, Jarvet J, Langel U, and Graslund A (2001) Secondary structure and position of the cell-penetrating peptide transportan in SDS micelles as determined by NMR. *Biochemistry* **40:**3141–3149.
Macura S and Ernst RR (1980) Elucidation of cross relaxation in liquids by two-dimensional NMR spectroscopy. *Mol Phys* **41:**95–117.
Marion D and Wühtrich K (1983) Application of phase sensitive two-dimensional correlated spectroscopy (COSY) for measurements of ^1H-^1H spin-spin coupling constants in proteins. *Biochem Biophys Res Commun* **113:**967–974.
Mazzoni MR, Taddei S, Giusti L, Rovero P, Galoppini C, D'Ursi A, Albrizio S, Triolo A, Novellino E, Greco G, et al. (2000) A $G\alpha_s$ carboxyl-terminal peptide prevents G_s activation by the A_{2A} adenosine receptor. *Mol Pharmacol* **58:**226–236.
Piantini U, Soerensen OW, and Ernst RR (1982) Multiple quantum filters for elucidating NMR coupling networks. *J Am Chem Soc* **104:**6800–6801.
Ralevic V and Burnstock G (1998) Receptors for purines and pyrimidines. *Pharmacol Rev* **50:**413–492.
Richard JP, Melikov K, Vives E, Ramos C, Verbeure B, Gait MJ, Chernomordik LV, and Lebleu B (2003) Cell-penetrating peptides. A reevaluation of the mechanism of cellular uptake. *J Biol Chem* **278:**585–590.
Slessareva JE, Ma H, Depree KM, Flood LA, Bae H, Cabrera-Vera TM, Hamm HE, and Graber SG (2003) Closely related G-protein-coupled receptors use multiple and distinct domains on G-protein α-subunits for selective coupling. *J Biol Chem* **278:**50530–50536.
Sunahara RK, Tesmer JJ, Gilman AG, and Sprang SR (1997) Crystal structure of the adenylyl cyclase activator $G\alpha_s$. *Science (Wash DC)* **278:**1943–1947.
Unterberger U, Moskvina E, Scholze T, Freissmuth M, and Boehm S (2002) Inhibition of adenylyl cyclase by neuronal P2Y receptors. *Br J Pharmacol* **135:**673–684.
Vanhauwe JF, Thomas TO, Minshall RD, Tiruppathi C, Li A, Gilchrist A, Yoon EJ, Malik AB, and Hamm HE (2002) Thrombin receptors activate G_o proteins in endothelial cells to regulate intracellular calcium and cell shape changes. *J Biol Chem* **277:**34143–34149.
Wishart DS, Sykes BD, and Richards FM (1991) Relationship between Nuclear Magnetic Resonance chemical shift and protein secondary structure. *J Mol Biol* **222:**311–333.
Wüthrich K (1986) *NMR of Proteins and Nucleic Acids*. John Wiley & Sons, New York.

Address correspondence to: Dr. Maria R. Mazzoni, Dip. di Psichiatria, Neurobiologia, Farmacologia e Biotecnologie, Via Bonanno 6, 56126 Pisa, Italy. E-mail: mariarm@farm.unipi.it